

Effect of Faradarmani Consciousness Field on Brain Metabolome via H-MRS with Focus on Energy-Related Metabolites

Mohammad Ali Taheri¹, Sara Torabi², Farid Semsarha^{3*}

* Corresponding author: Farid Semsarha Tel.: +98-9121786577

Email: Semsarha@ut.ac.ir

1. Sciencefact R&D Department, Cosmointel Inc.
Research Center, Ontario, Canada

2. Department of Plant Biology, School of Biology, College
of sciences, University of Tehran, Tehran, Iran

3. Institute of Biochemistry and Biophysics (IBB),
University of Tehran, Tehran, Iran

DOI: <https://doi.org/10.61450/joci.v4i19.224>

Abstract

This study investigates the effects of the Faradarmani Consciousness Field on metabolite changes, with a focus on potential alterations in energy metabolism. A previous study using fMRI revealed that certain brain regions of trained individuals, referred to as Faradarmangars, become activated or deactivated during the task state or under the influence of this Consciousness Field. Proton magnetic resonance spectroscopy (¹H-MRS), as a non-invasive method, enables the evaluation of brain function and metabolic changes under the influence of the Faradarmani Consciousness Field. Based on the obtained results, a specific reduction in the need for and consumption of ATP molecules and related metabolic pathways, along with a significant change in brain cell energetics—particularly in the activated region—can be identified. In this context, increases in lactate, ascorbate, and the macromolecule MM09 in this area may support enhanced metabolic processes recorded by fMRI. On the other hand, in the deactivated region, despite no statistically significant change, decreasing trends in glycerophosphorylcholine (GPC) and ascorbate, along with increasing trends in Pch, glutamate, and Lip13b, reflect a distinct metabolic response compared to the activated brain region. Further investigation of energy-related metabolites, particularly ATP, in the rest-task comparison under the influence of the Faradarmani Consciousness Field using phosphorus MRS is planned by the authors.

Keywords: MRS; Energy; Faradarmani Consciousness Field, Brain Metabolome

Introduction

The human brain is one of the most complex and vital organs, governing not only basic physiological processes but also higher cognitive functions such as perception, emotion, and consciousness. Understanding its intricate workings has long been a central goal of neuroscience. Over the past decades, considerable progress has been made in uncovering the biochemical and functional dynamics of the brain (Pessoa 2014). Among several standard neuroimaging techniques, Magnetic Resonance Spectroscopy (MRS) has emerged as a powerful non-invasive tool for probing brain metabolism, providing insights into the biochemical underpinnings of neural function and dysfunction (Yen et al., 2023).

In parallel with these scientific developments, increasing attention has been given to the influence of mind-based and consciousness-related phenomena on the brain and body (Schwartz et al., 2005). Generally, two dominant perspectives exist regarding the emergence of consciousness. The prevailing view in neuroscience holds that consciousness is locally generated by the brain through neuronal activity (Koch et al., 2016). In contrast, the concept of non-local consciousness suggests that consciousness extends beyond the physical boundaries of the brain. This perspective is supported by a range of interdisciplinary studies, including research in quantum physics, near-death experiences, telepathy, and other consciousness-related anomalies (Dossey, 2014; Lohrey and Boreham, 2020; Wahbeh et al., 2022).

It is worth noting that recent research highlights that consciousness is fundamentally distinct from attention. While attention is regarded as a basic cognitive function—one of the earliest evolutionary developments of the nervous system—consciousness encompasses a broader and more intricate set of processes. It underlies essential functions such as decision-making, voluntary control of actions, future planning, memory recall, and the construction of self-awareness. Neuroscientific evidence suggests

that phenomenal consciousness is primarily linked to synchronized activity across the temporo-parietal-occipital regions, whereas attention is governed by fronto-parietal networks that selectively amplify specific aspects of experience (Nani et al., 2019).

In Taheri's approach, consciousness is regarded as a fundamental element of the universe, from which information, matter, and energy originate. Within this framework, the human brain and nervous system are not producers of consciousness but rather act as detectors—analogue to hardware—responsible for receiving and processing information. This system operates in coordination with the mind, which functions as a kind of software that provides information indices necessary for the emergence of consciousness. When brain function is impaired, such as in the case of injury, the system's ability to receive and process information is disrupted—much like a damaged antenna failing to detect signals—thereby hindering conscious experience.

In this viewpoint, there are various T-Consciousness Fields (TCFs) with different functions. The current study used Faradarmani Consciousness Field as one of these non-physical TCFs. The application of this field is not based on learned mental techniques like breath control, sustained attention, or visualization—common in practices such as meditation or mindfulness. Instead, the engagement with TCFs is initiated by a brief moment of attention, typically lasting only a few seconds, with no further mental effort required from the participant. Therefore, any observed physiological or metabolic changes cannot be attributed to intentional mental activity or cognitive effort, as none are employed. Moreover, these findings support the hypothesis that the brain, acting as a detector, can receive information from Faradarmani Consciousness Field, and that such interactions may manifest as measurable changes in the brain's metabolic profile.

Method

MRI was performed on a 3.0-T clinical scanner (Magnetom Prisma, Siemens Medical Solutions, Erlangen, Germany) with a gradient strength of 40 mT/m. A body-connected coil enabled the transmission of excitation. Specifically, a ^1H phased-array head coil (125 MHz) was used for signal detection (Siemens Rapid Biomedical, Germany).

After acquiring scout images of the subjects, a T2-weighted imaging protocol was performed in axial and coronal planes to capture data from the regions of interest. The MRI protocols were also followed for the MRS experiments. Data acquisition was conducted in two phases: similarly to previous steps, from baseline up to 15 minutes before the onset of treatment (rest phase), and immediately after the initiation of the treatment up to 15 minutes (task phase).

The T2-weighted imaging protocol was based on a standard spin-echo sequence with the following parameters: TR/TE = 5000/77 ms, NEX = 2, FOV = $4 \times 4 \text{ cm}^2$, matrix size = 256×256 , and slice thickness = 1 mm. Prior to performing MRS, a voxel of $1 \times 1 \times 1 \text{ cm}^3$ was defined in each of the three target regions for each subject. Following manual shimming and water suppression adjustment, short-echo proton MR spectra with high signal quality were acquired using the PRESS technique (TR/TE = 6000/135 ms, 156 acquisitions).

Before starting the MRS test, water suppression was performed using second-order shimming and a Chemical Shift Selective (CHESS) pulse sequence. At the end of the MRS experiment, the reference water signal was acquired by disabling water suppression to allow for metabolite concentration calibration. The described MRI and MRS protocols were conducted similarly both before and after the treatment process. Rest and task imaging were performed sequentially without moving the subjects and with their eyes completely closed during both phases.

Experimental design

Based on fMRI data from previous studies, in order to investigate metabolic changes in the activated and deactivated brain regions of Faradarmangars, three regions were selected: one containing an activated area (right Precentral Gyrus), one containing a deactivated area (right Superior Temporal Gyrus), and a third region with similar dimensions located between the activated and deactivated areas, which, according to the obtained data, does not show activation or deactivation in response to the Faradarmani Consciousness Field (Figure 1). The third region was chosen to serve as a negative control for comparing potential metabolic changes with the other two regions. Images of the selected regions and the MRS spectra obtained during the rest state are presented in Figures 2 to 4.

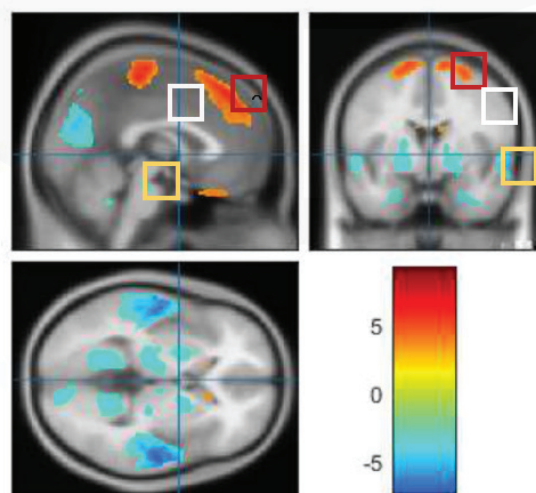


Figure 1. Three selected regions based on fMRI data. Red box: Activated region, Yellow box: Deactivated region, White box: Neither activated nor deactivated region (Taheri et al., 2022).

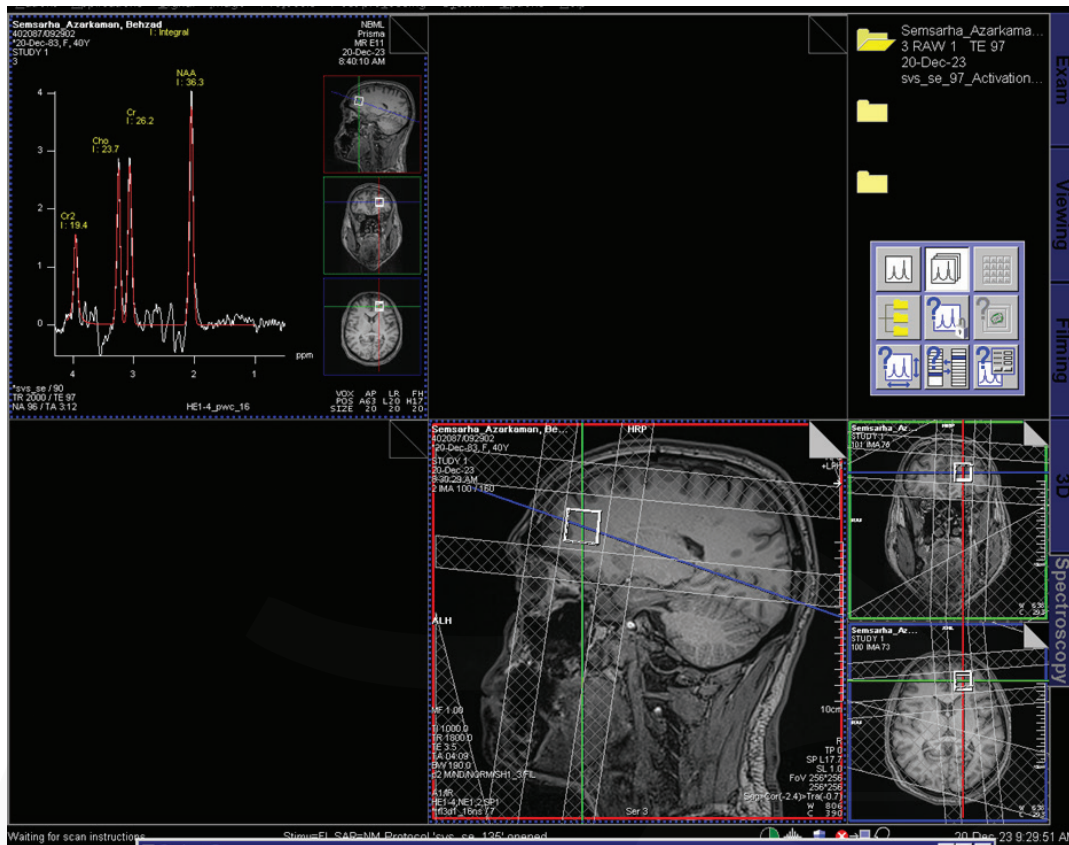


Figure 2. T2-weighted MR image of one of the study subjects, showing the placement of the MRS voxel on the selected activated region under Faradarmani Consciousness Field treatment, along with the proton spectrum obtained in the rest state.

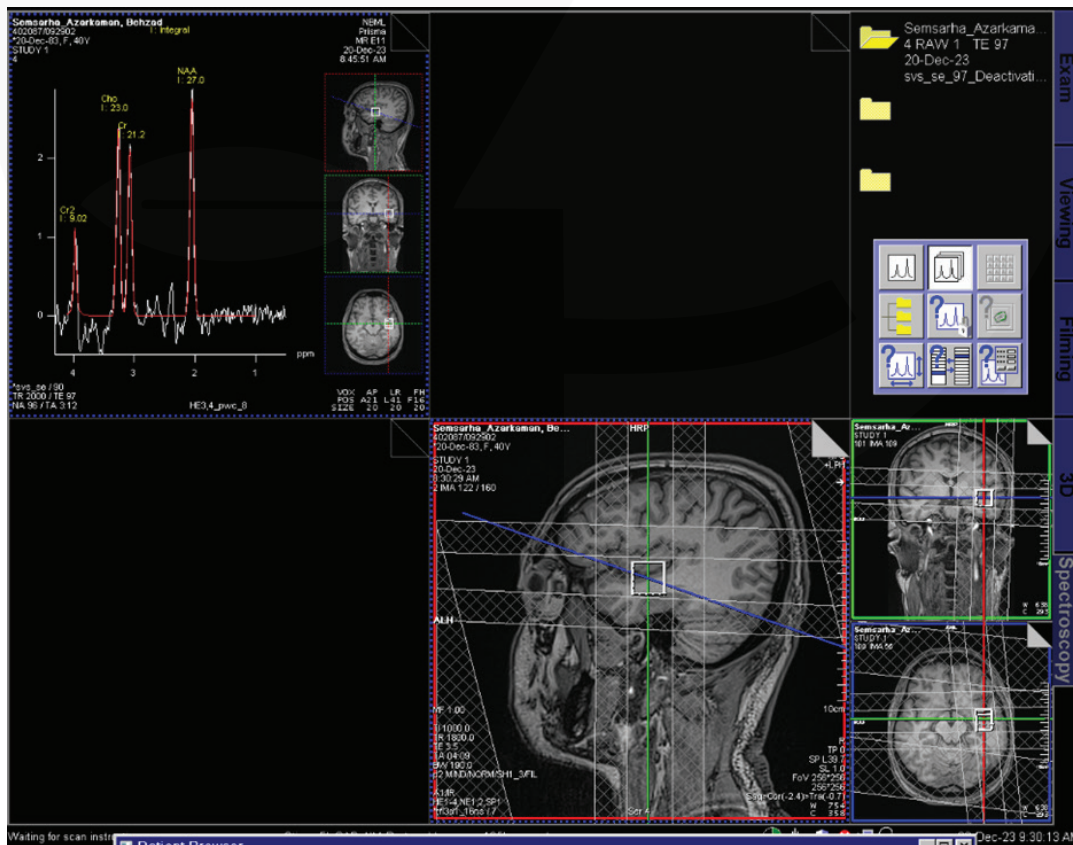


Figure 3. T2-weighted MR image of one of the study subjects, showing the placement of the MRS voxel on the selected deactivated region under Faradarmani Consciousness Field treatment, along with the proton spectrum obtained in the rest state.



Figure 4. T2-weighted MR image of one of the study subjects, showing the placement of the MRS voxel on the selected neither activated nor deactivated region during Faradarmani Consciousness Field treatment, along with the proton spectrum obtained in the rest state.

Analysis of the MR spectrum

The volume of interest (VOI) for the MRS experiments was drawn on T2-weighted images. We attempted to create identical VOIs for the three regions across different subjects to ensure similar coverage of the target areas in each individual. Each spectrum corresponding to the selected regions was analyzed using a Java-based graphical user interface. This interface, used for the MRUI quantification package, contains a basic knowledge base of 57 peaks associated with at least 34 different metabolites. Metabolite concentrations were determined relative to the water signal used as a reference. Therefore, all amplitudes in each MR spectrum were expressed semi-quantitatively. It is also worth mentioning that the advanced method for accurate, robust, and efficient spectral fitting (AMARES) was used for quantification (Vanhamme et al., 1997).

The Application of Faradarmani Consciousness Field

In the present study, a population-level MRS analysis was conducted on Faradarmangars, comparing metabolite changes in selected brain regions during the task and rest phases. The task refers to the activity during which a Faradarmangar personally connects to the Cosmic Consciousness Network. This study was approved by the Ethics Committee of Iran University of Medical Sciences (Approval ID: IR.IUMS.REC.1402.940).

Thirty healthy adult participants (mean age: 42 ± 7 years), all with no history of neurological or psychiatric medication use in the six months prior to the test day, were included in the study group. Of these participants, 40% were male ($n = 12$) and 60% were female ($n = 18$). The design of the studies conducted using the MRS technique included a 15-minute rest phase (prior to connection with the field) and a 15-minute

task phase, representing the state of connection with the Faradarmani Consciousness Field (initiated immediately after the rest phase). Further details about each phase of the study in chronological order are as follows:

- 1. Rest:** A 15-minute initial phase in which Faradarmangars were instructed, while inside the MRI scanner, to keep their eyes closed and remain relaxed and stress-free, without engaging with any Consciousness Fields. The purpose of this phase was to obtain control data, representing the baseline state before connection with the field. This baseline plays a critical role in constructing population-level control data or "pre-connection" references.
- 2. Task:** In this study, the second 15-minute phase—immediately following the rest phase without any temporal gap—is referred to as the task phase. In this phase, the individuals establish a connection with the Faradarmani Consciousness Field. This connection is initiated solely by the participants themselves upon hearing a predefined beep, which they had been informed in advance signals the beginning of the connection.

Data Analysis

The data obtained from this study were statistically analyzed using GraphPad Prism software (version 9). One-way analysis of variance (ANOVA) was used to assess differences in metabolite levels between the rest and task phases. For each group's MRS dataset, the Wilcoxon test was applied at a 5% significance level to compare changes in metabolite concentrations between these two phases. Pearson correlation analysis and the calculation of correlation coefficients (r) were conducted using a two-tailed p-value. A p-value of less than 0.05 was considered statistically significant.

Results and Discussion

N-acetyl-aspartate

Figure 5 illustrates the changes in NAA¹ and NAAG² in both activated and inactivated regions under the influence of Faradarmani Consciousness Field. NAA is one of the most important compounds assessed in MRS and is identified at the chemical shift of 2.0 ppm. As observed, in both the activated and non-activated brain regions, the population average of NAA shows a decreasing trend, in contrast to NAAG. However, a negative Pearson correlation between the decreasing levels of NAA and the increasing levels of NAAG is observed only in the activated brain region, not in the non-activated one. (A positive correlation between NAA and NAAG in the non-activated region suggests the metabolic consumption of NAAG.) This indicates that a reciprocal (seesaw-like) pattern of change between these two metabolites can be claimed for the activated region. The reciprocal increase in NAAG and decrease in NAA suggests that NAAG is not being hydrolyzed into NAA (Barker and Lin, 2006; Oz et al., 2014).

1 N-Acetylaspartate

2 N-Acetylaspartylglutamate

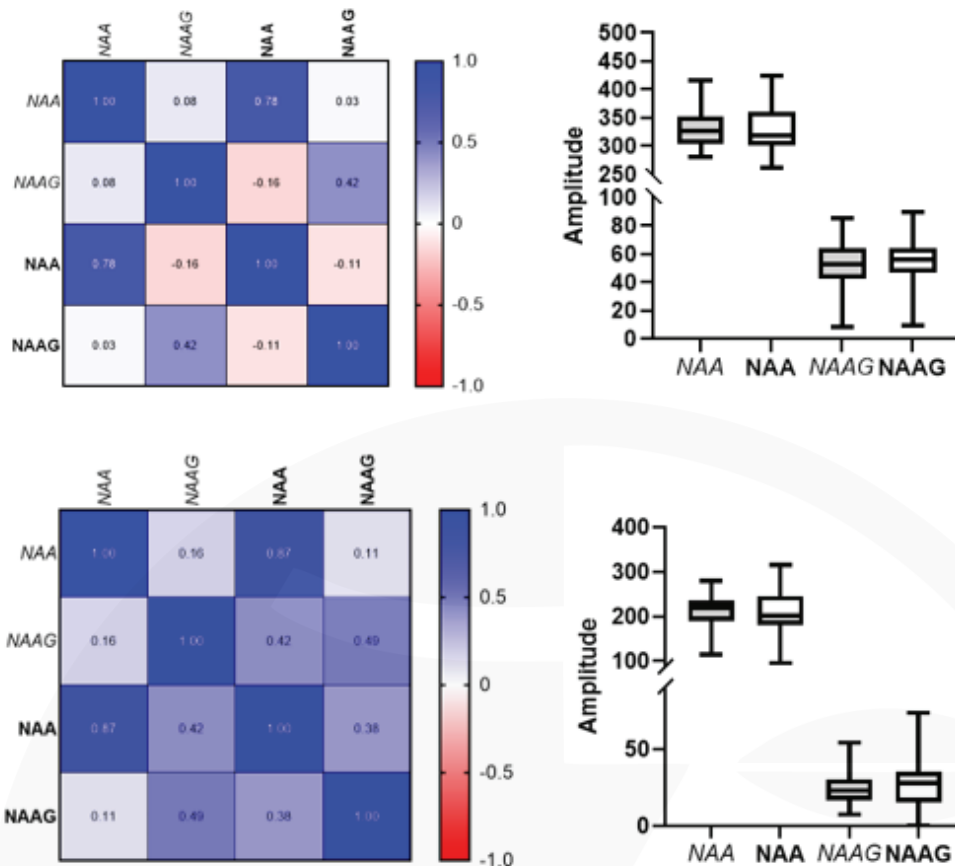


Figure 5. Box plot of changes in aspartate metabolite levels along with their Pearson correlations under rest and task conditions in the activated brain region (top) and the non-activated brain region (bottom). *Italic*: rest. **Bold**: task.

The brain is unique among organs in many ways, including its lipid synthesis mechanisms and energy production. The nervous system-specific metabolite N-acetylaspartate (NAA)—synthesized from aspartate and acetyl-CoA in neurons—is a key molecule underlying these distinct biochemical features of CNS metabolism. During early postnatal CNS development, the expression of lipogenic enzymes in oligodendrocytes, including aspartoacylase (ASP), which breaks down NAA, increases in parallel with the elevated production of NAA in neurons (Moffett et al., 2007).

This molecule also plays additional roles, including a bioenergetic function in neuronal mitochondria. Its production occurs in the mitochondria of neurons and is ATP-dependent (Moffett et al., 2007; Ariyannur et al., 2008). NAA is the acetylated form of the amino acid aspartate and is found in high concentrations in neurons, serving as a marker of neuronal viability. Therefore, in any process that leads to neuronal loss—such as high-grade tumors,

and neurodegenerative diseases—NAA levels decrease (Rigotti et al., 2007).

Reduction of NAA in both activated and deactivated brain regions of Faradarmani practitioners—despite the physiological health of the brain—indicates that the observed phenomenon in the brain is independent of this metabolite and intracellular ATP levels. Given the role of aspartate in ATP production, a decrease in NAA indirectly leads to reduced ATP levels. NAA reflects neuronal viability and neural osmotic regulation, while NAAG plays a role in glutamate release (a proposed pathway in the deactivated region based on observed changes in glutamate), neuronal protection, and synaptic plasticity (Castellano et al., 2012).

Total choline

Figure 6 shows a comparison of changes in total choline levels in the activated and deactivated brain regions of Faradarmangars. The comparison

of total choline levels between the task and rest states in the activated and deactivated brain regions of Faradarmangars is also presented in Table 1. Choline is an essential biomolecule for all cells and is required for the synthesis of phosphatidylcholine and sphingomyelin, which are major components of the plasma membrane (Zeisel et al., 2009).

The formation of new cell membranes requires a rate-limiting step of choline uptake followed by phospholipid biosynthesis (Inazu, 2019). Choline is also a precursor to the neurotransmitter acetylcholine and the methyl donor betaine, both of which play roles in several critical biological functions (Dymek et al., 2024).

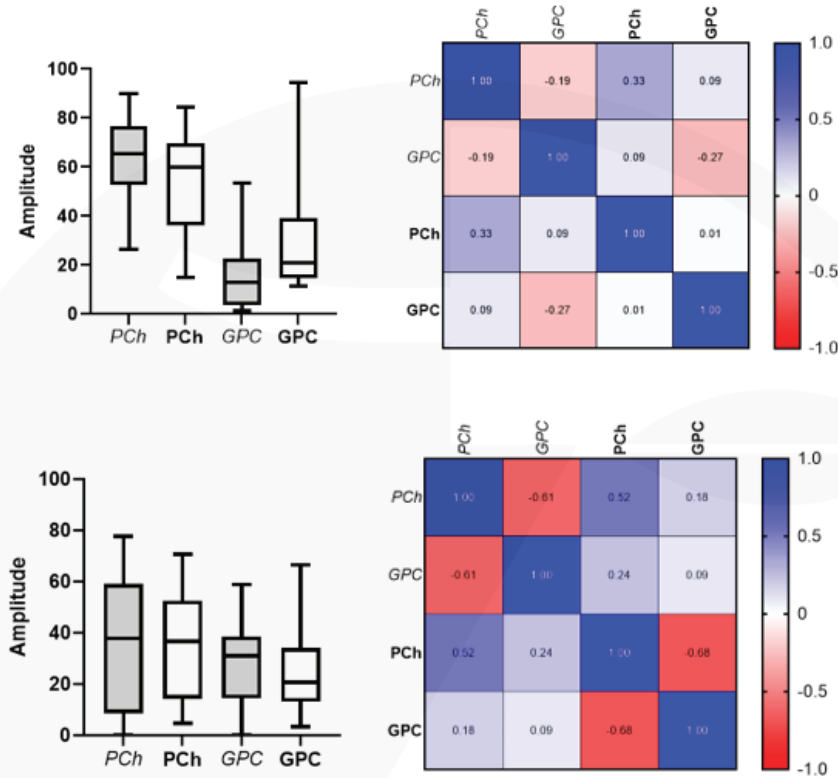


Figure 6. Box plot of changes in choline metabolite levels (phosphocholine and glycerophosphocholine) along with their Pearson correlation in the rest and task conditions for the activated brain region (top) and the deactivated brain region (bottom). *Italics*: Rest. **Bold**: Task.

Table 1. Total choline levels in rest and task conditions of activated and deactivated brain regions of Faradarmangars. *Italic*: rest; **Bold**: task.

	Activation		Deactivation	
	<i>PCh+GPC</i>	PCh+GPC	<i>PCh+GPC</i>	PCh+GPC
Minimum	14.67	28.23	15.7	16.8
Maximum	84.61	89.76	80.0	77.4
Range	69.94	61.53	64.3	60.6
Mean	62.19	66.05	48.3	48.1
Std. Deviation	19.51	15.57	16.3	18.3
Std. Error of Mean	4.364	3.482	3.39	3.82

The absence of change and the increase in total choline levels as a result of the task, respectively, in the deactivated and activated brain regions of Faradarmangars, indicate no limitation or deficiency of the choline metabolite in these areas. On the other hand, the decreasing trend of phosphocholine and the increasing trend of glycerophosphocholine in the activated brain region suggest a relative halt in the cycle of phosphocholine production from choline, effectively indicating inhibition of the enzyme choline kinase, which functions by consuming ATP. Moreover, the negative correlation between GPC levels during the task and rest conditions—considering the increase in GPC during the task—indicates a reduction of this metabolite during rest, suggesting its redistribution through metabolic pathways outside the choline–GPC cycle (i.e., acetylcholine synthesis: signaling; phosphatidylcholine synthesis: cell membrane formation).

Additionally, changes in total choline levels in the deactivated brain region of Faradarmangars show a phosphocholine trend similar to that of the activated region, though with a smaller decrease, and an opposite trend for GPC compared to the activated region. This observation, alongside the relative decrease in phosphocholine, suggests that GPC is entering a pathway outside the GPC–choline cycle (similar to the rest condition in the activated region), specifically into pathways related to acetylcholine and phosphatidylcholine synthesis.

The decrease in phosphocholine in both the activated and deactivated brain regions of Faradarmangars, despite no apparent limitation in choline, may indicate reduced activity of the enzyme choline kinase—possibly due to a decreased availability of ATP. On the other hand, based on these data, the key metabolite distinguishing between the activated and deactivated brain regions of Faradarmangars is the GPC molecule, which shows an increase in the activated regions—exactly opposite to

the changes in its concentration observed in the deactivated regions.

Total creatine

The changes in creatine metabolite are shown in Figure 7 and Table 2. Creatine and its phosphorylated derivative, phosphocreatine (PCr), are essential for sustaining ATP levels in energy-intensive tissues like skeletal muscle, the heart, and the brain (Bonilla et al., 2021). An important point in comparing the activated and deactivated regions in the box analysis is the inverse relationship in metabolite changes between these regions in the brains of Faradarmangars, which confirms the contrasting types of activity in these areas. In the activated region, the decreasing trend of phosphocreatine in both the mean and distribution of test samples contrasts with the behavior of the creatine metabolite in the same samples. Similar to choline metabolites, the phosphorylated form of creatine decreases in comparison to its base form in these regions. In fact, the Faradarmani Consciousness Field treatment leads to a reduction in the phosphorylated form of creatine, which depends on intracellular ATP. The negative correlation between creatine and phosphocreatine observed during rest ($r = -0.49$) is also seen during the task, but with a stronger negative correlation ($r = -0.76$). In contrast, in the deactivated brain region of Faradarmangars, the level of phosphocreatine shows an increasing trend, unlike creatine.

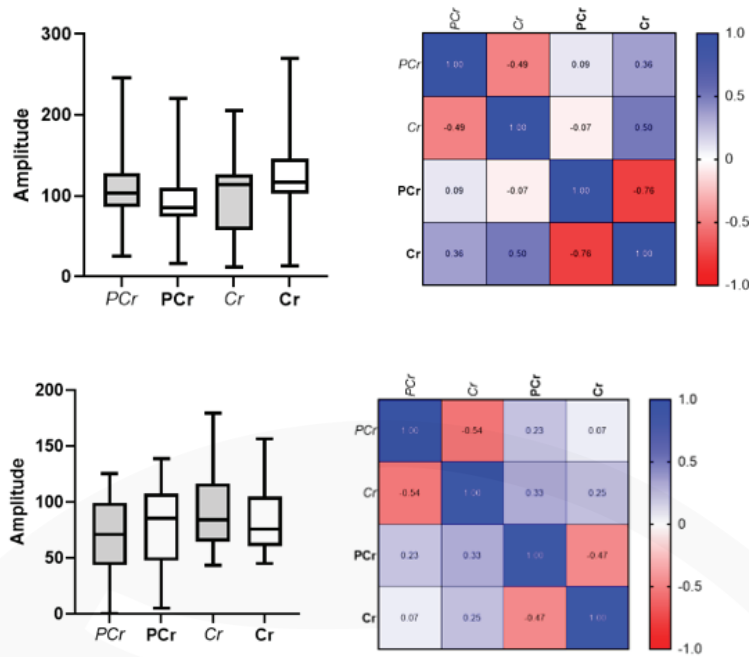


Figure 7. Comparison of creatine metabolite levels in the box analysis and Pearson correlation assessment in task (**Bold**) and rest (*Italic*) from the activated (top) and deactivated (bottom) brain regions of Faradarmangars. *Italic*: rest; **Bold**: task.

Table 2 presents the changes in total creatine levels in the rest and task conditions of activated and deactivated brain regions of Faradarmangars. Considering the lack of significant changes in total creatine levels between the rest and task conditions in both the activated and deactivated regions, the observed decrease in the activated region suggests a

reduction in ATP availability or demand during task condition in this area. In contrast, in the deactivated regions, phosphorylated creatine increases and, similar to the GPC metabolite, plays a role as a distinguishing metabolite between the activated and deactivated brain regions of Faradarmangars.

Table 2. Total creatine levels in the rest and task conditions of activated and deactivated brain regions of Faradarmangars. *Italic*: rest; **Bold**: task.

	Activation		Deactivation	
	<i>Cr+PCr</i>	Cr+PCr	<i>Cr+PCr</i>	Cr+PCr
Minimum	68.76	73.74	76.2	18.5
Maximum	286.5	265.7	221	217
Range	217.7	191.9	145	198
Mean	203.1	203.0	159	153
Std. Deviation	46.20	41.06	35.1	47.8
Std. Error of Mean	10.33	9.181	7.32	9.97

Amino acids

Changes in the levels of the amino acids glutamate and glutamine, as well as various amino acid metabolites, are presented in Figure 8. As observed, the changes in amino acids between the rest and task conditions in both activated and deactivated regions are not

significant. However, among all amino acids, glutamate and glutamine (with glutamate being predominant) show the highest levels across all samples. Additionally, in the deactivated regions, there is a general increasing trend of glutamate during the task compared to the rest condition.

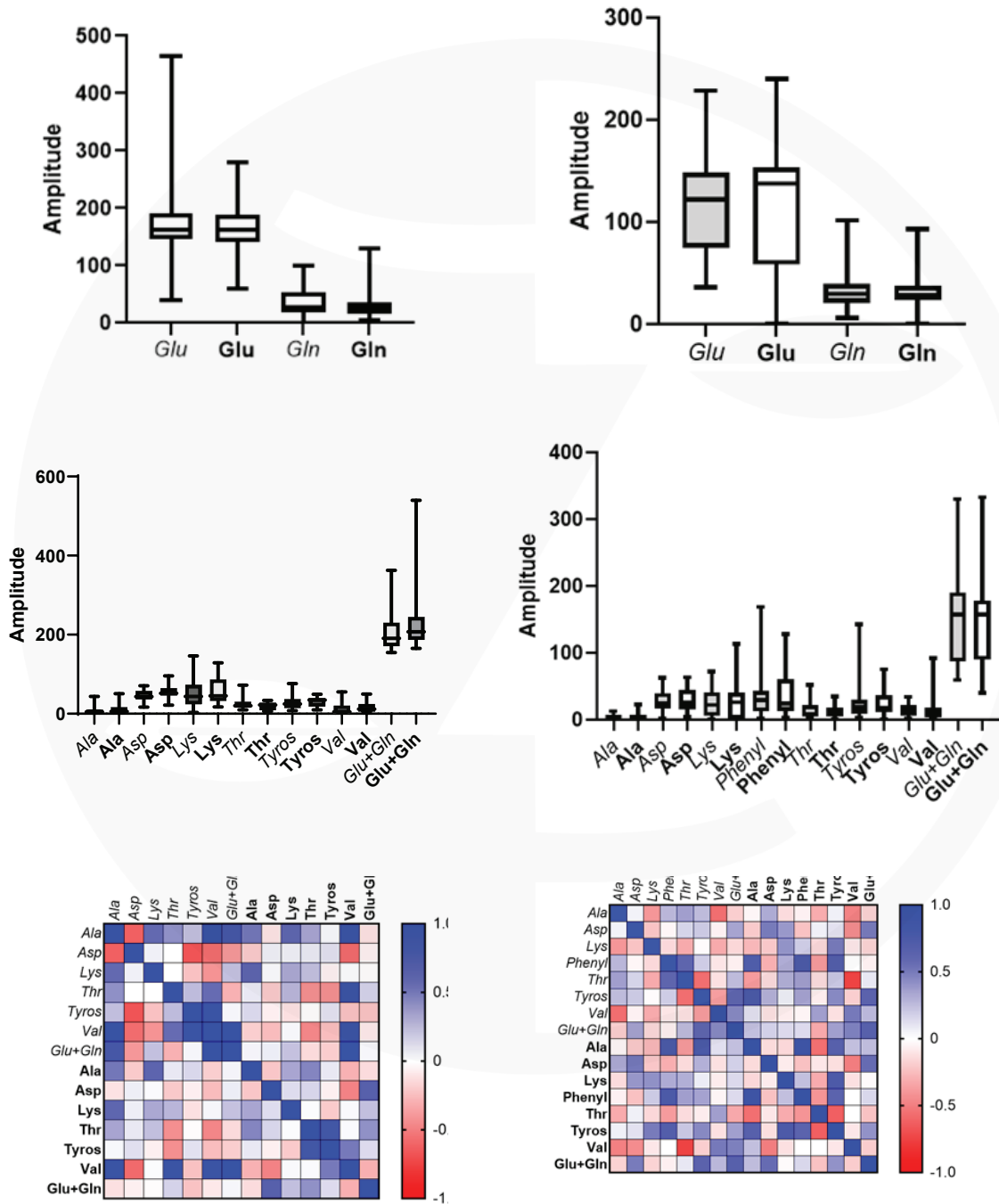


Figure 8. Comparison of glutamate and glutamine amino acid levels, along with various amino acid metabolites in the box analysis, and their Pearson correlation in task and rest conditions of the (left) activated and (right) deactivated regions. *Italic*: rest; **Bold**: task.

Other metabolites 1

A set of metabolites categorized under the conventional group “Other Metabolites 1” is compared here between rest and task conditions in the activated and deactivated brain regions. As shown in Figure 9, a significant increase in ascorbate is observed under task conditions, accompanied by a positive correlation with GABA. On the other hand, in the deactivated regions, although no significant changes in metabolite levels are detected between rest and task conditions, the trend of ascorbate changes is notably opposite to that in the activated region. In fact, alongside GPC and PCh, ascorbate also exhibits distinct patterns of change between the activated and deactivated brain regions.

Ascorbate, also known as vitamin C, is one of the major non-enzymatic antioxidants present in high concentrations in the human central nervous system (Olufunmilayo et al., 2023). The maintenance of its millimolar-level homeostatic concentration highlights its important role in the brain, which is particularly vulnerable to oxidative damage (Rice, 2000). Several studies have shown that oxidative stress contributes to impaired brain function during normal aging and represents a constant risk factor for the nervous system and the onset of related diseases (Trofin et al., 2025).

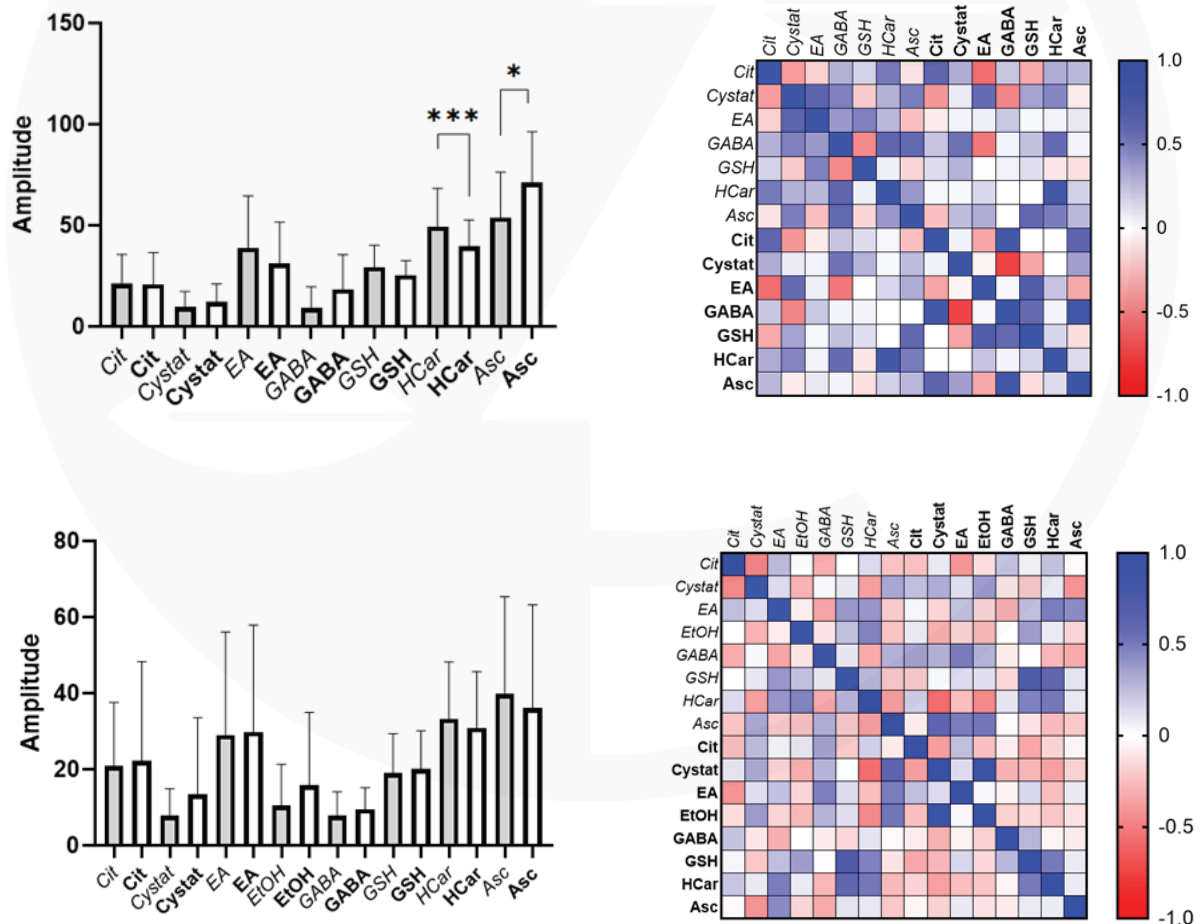


Figure 9. Comparison of various metabolite levels in the activated (top) and deactivated (bottom) regions of test and control samples, presented as box analyses along with their Pearson correlation. *Italic*: rest; **Bold**: task.

Homocarnosine is a unique dipeptide composed of GABA and histidine found in the brain, present in significantly higher concentrations in the human brain (0.3–1.6 mmol/L) compared to other mammals (<0.07 mmol/L) (Hetherington et al., 2000). It is synthesized in the cytosol of a subclass of GABA-producing neurons by the enzyme homocarnosine synthetase (Veiga-da-Cunha et al., 2014). The substrates of the enzyme are histidine, GABA, and ATP; its products include homocarnosine, ADP, free magnesium, and a hydrogen ion (Hetherington et al., 2000).

As shown in Figure 9, the significant decrease in homocarnosine—produced through the reaction of the substrates GABA, histidine, and ATP by the enzyme homocarnosine synthetase—is notable. Based on the findings in this section,

inhibition of homocarnosine synthetase is suggested as a result of the Faradarmani Consciousness Field treatment, likely due to reduced ATP availability, since there appears to be no limitation in GABA or amino acids such as histidine.

Other metabolites 2

Another set of metabolites, categorized under the second group of "Other Metabolites 2," has been compared in this section under rest and task conditions in the activated and deactivated brain regions. As shown in Figure 10, the increase in lactate in the task condition from the activated region is the only significant and notable change among the compared metabolites.

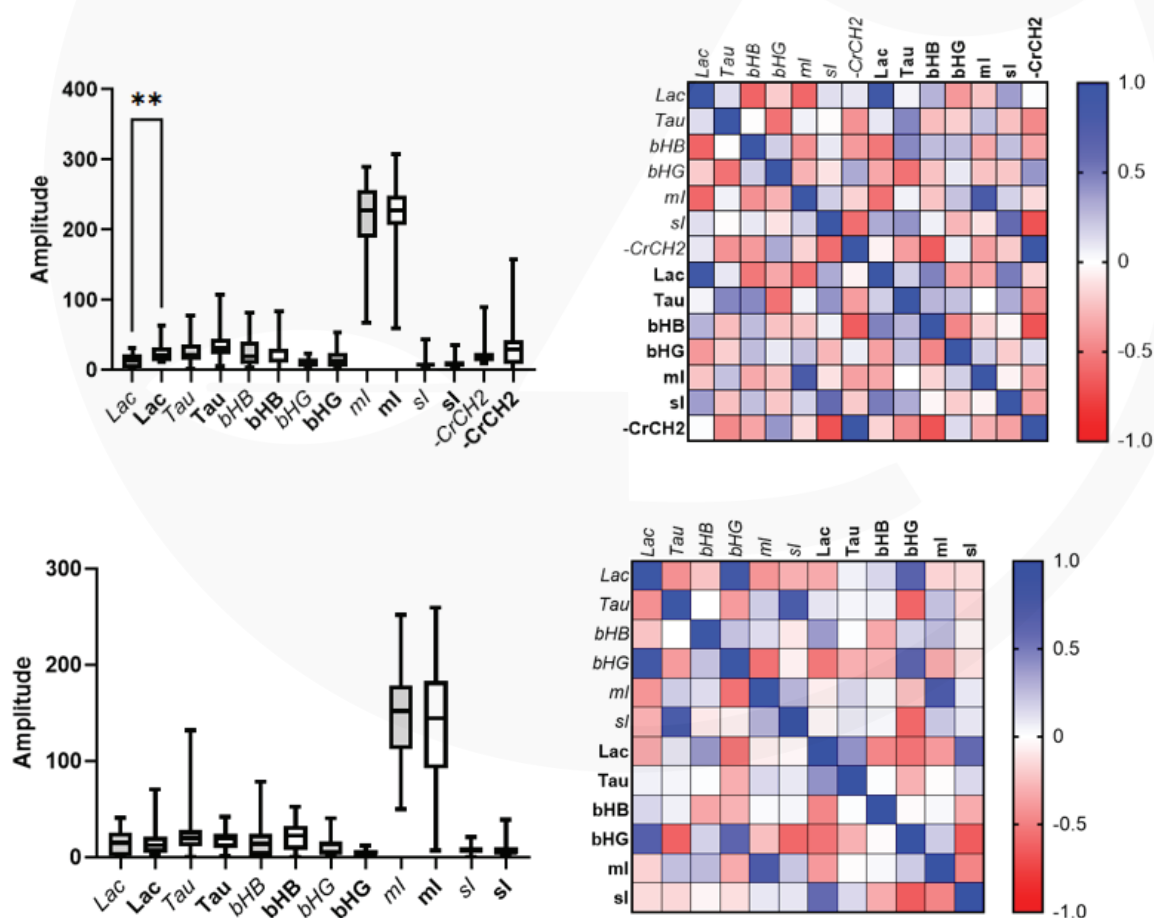


Figure 10. Comparison of selected metabolite levels presented as box plot analyses along with their Pearson correlations in rest and task conditions from activated (top) and deactivated (bottom) brain regions. *Italic*: rest; **Bold**: task.

During fetal brain development, lactate levels increase significantly from the mid-gestation stage onward. This highlights the vital role of lactate in brain growth and neural differentiation (Nordström et al., 2001). In the brain, astrocytes—a type of glial cell—primarily produce lactate from glucose or glycogen in response to neural activity signals. Neurons and astrocytes exhibit a strong metabolic partnership, with lactate being transferred from astrocytes to neurons to meet neuronal energy demands. Beyond supplying energy, lactate also modulates neural functions such as excitability, plasticity, and memory consolidation. In fact, lactate is increasingly recognized as a signaling molecule in the brain, linking metabolism, substrate availability, blood flow, and neural activity (Alberini et al., 2018; Beard et al., 2022; Benarroch, 2024).

Among this category of metabolites, myo-inositol exhibits the highest concentration under both task and rest conditions in both regions, with an overall trend showing opposite patterns of change between the activated and deactivated areas (Figure 10). Myo-inositol is a precursor of phosphatidylinositol (the main inositol-containing phospholipid) and phosphatidylinositol 4,5-bisphosphate (a key molecule in cellular signal transduction), and it also plays a significant role in osmotic regulation (Chhetri, 2019). This metabolite shows an increase in the activated brain region of Faradarmangars.

Macromolecular Metabolites

Various macromolecular metabolites, categorized based on their detection frequency, are compared in this section.

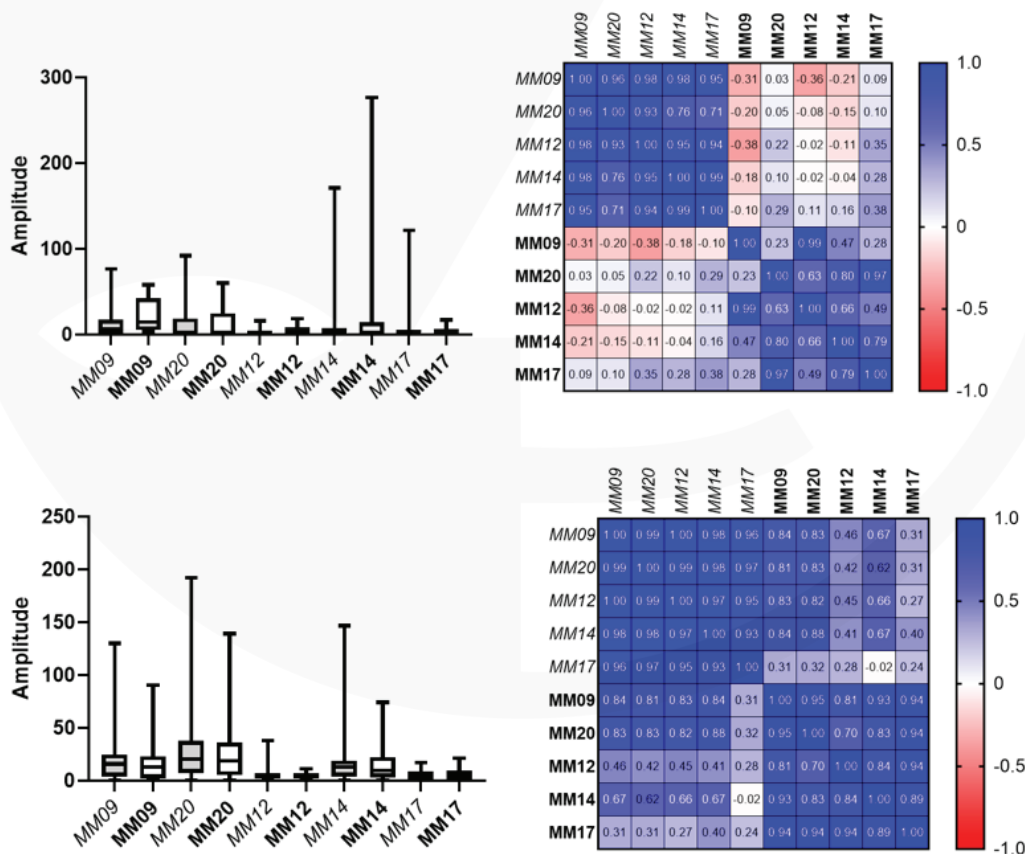


Figure 11. Changes in various macromolecules in task and rest conditions are shown through boxplot analysis and Pearson correlation in the activated (top) and deactivated (bottom) brain regions of Faradarmangars. *Italic: rest. Bold: task.*

As shown in Figure 11, a difference is observed between task and rest conditions regarding macromolecular metabolites in the activated region. In fact, as illustrated by the Pearson correlation analysis, the contrast in metabolite trends between task and rest is reversed, indicating divergent alterations in macromolecular metabolite levels. Although a similar difference is also detectable in the deactivated region, it is not as pronounced as in the activated area. Notably, a rising trend in MM09 is evident in the activated brain region. As seen in the Pearson correlation, the negative correlation between task and rest values in the activated region clearly indicates the influence of the Consciousness Field treatment. Specifically, MM09 in the task condition shows a negative correlation compared to all macromolecular types in the rest group, reflecting an upward trend in the task group relative to the rest.

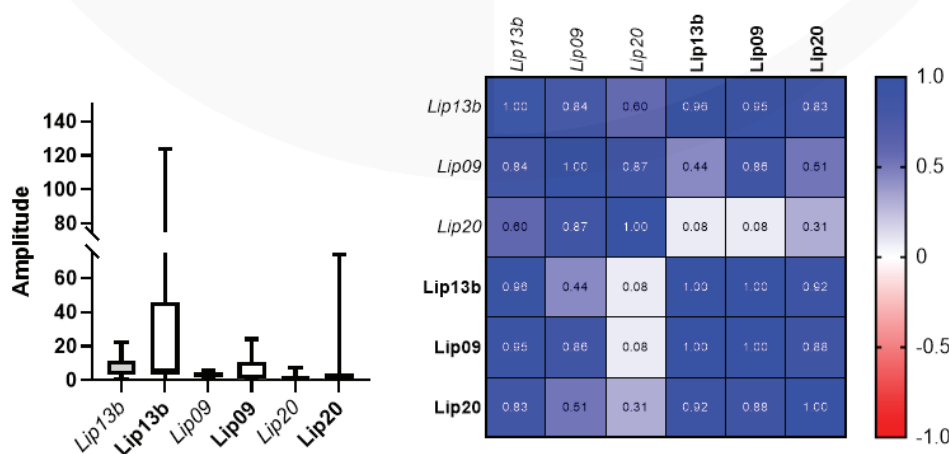
Altered macromolecular (MM) signal intensity—such as that seen in aging or neurological disorders—has been associated with changes in total protein concentration or mobility (Cudalbu et al., 2021; Akiyama et al., 2021). However, in the present study, participants were healthy adults aged 42 ± 7 years, and the Faradarmani Consciousness Field (FCF) was applied for a brief duration of only 15 minutes. Given these conditions, the observed increase in MM09 cannot plausibly be attributed to pathological or age-related processes. Instead, this short-term modulation during the task phase likely

reflects an FCF-induced shift in intracellular protein dynamics or glial–neuronal interactions, suggesting a functional, state-dependent neurochemical response that merits further investigation.

Lipid Metabolites

The comparison of lipid metabolites in active and inactive regions of the brain resulted in analyzable data in Magnetic Resonance Spectroscopy (MRS), which is presented in Figure 12. As seen in the charts, the average value changes in the active brain regions do not show any significant variation or trend; furthermore, the correlation of value changes is generally positive, with the exception of Lip20, which shows no correlation with other lipids as a result of the task.

On the other hand, in the inactive region of the brain, notable changes are observed. For Lip13b, the highest lipid level among the samples is seen in the inactive brain region, and during the task condition, an increasing trend in its average is observable. Additionally, this lipid shows a negative correlation with the levels of other lipids in both task and rest conditions, indicating a reverse pattern—such that with an increase in Lip13b under task conditions, the other lipids tend to decrease. This reflects a distinct pattern in the Faradarmani-treated state compared to the rest condition in the inactive brain region.



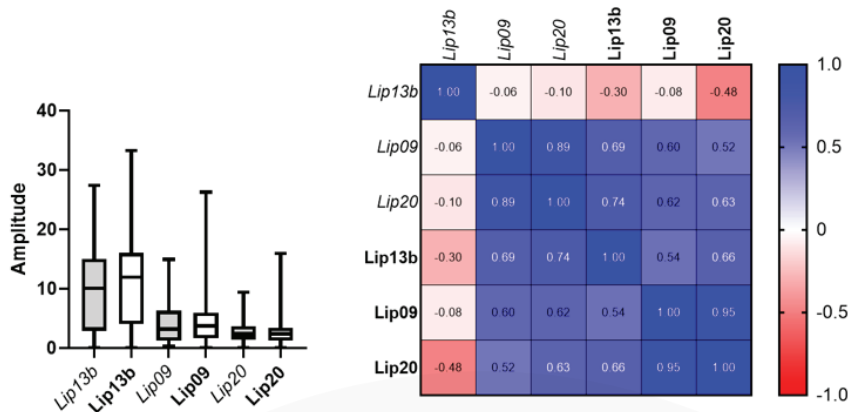
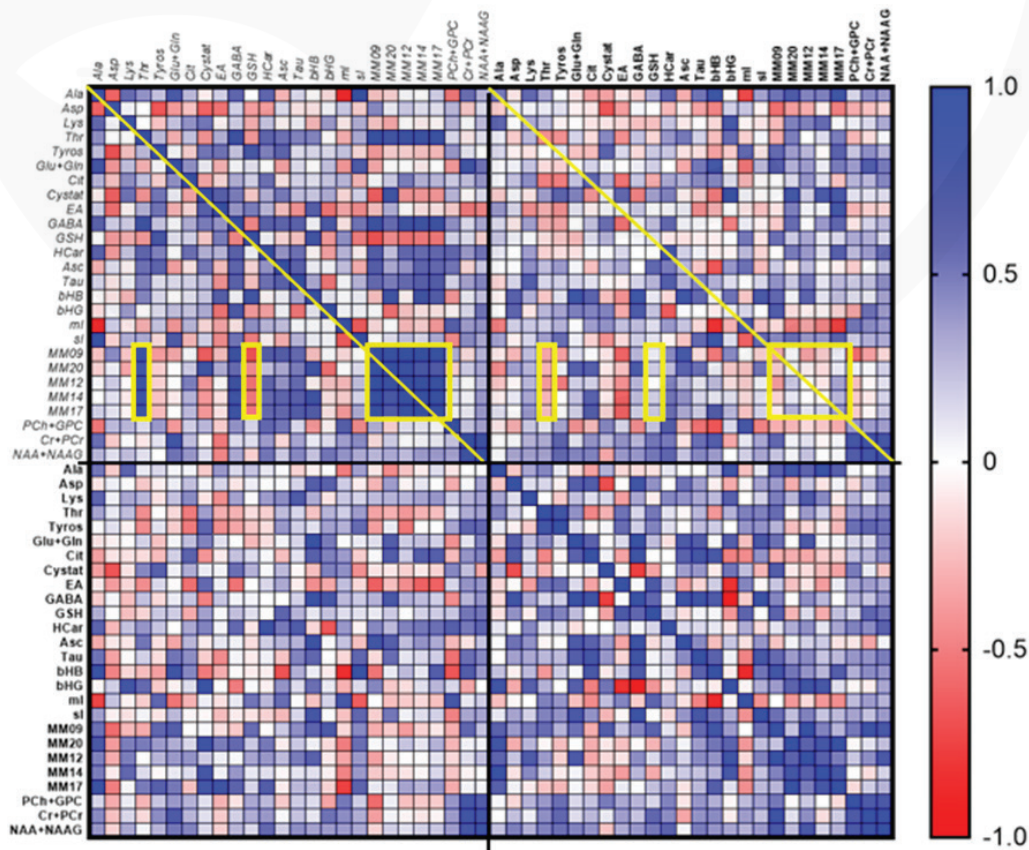


Figure 12. Changes in lipid metabolites under task and rest conditions in box plot analysis and Pearson correlation in the active (top) and deactivated (bottom) brain regions of Faradarmangars. *Italic*: rest. **Bold**: task.

Combined Correlation Analysis of All Metabolites

Finally, in the Figure 13, the overall Pearson correlation profile of changes in the activated and deactivated brain regions of Faradarmangars during rest and task is presented. As observed, the Pearson correlation analysis of all metabolites together in the activated and deactivated brain regions reveals changes in the metabolite value profiles. In both activated and deactivated regions, the perfect correlation (+1) between

identical metabolites generally disappears (yellow lines in Figure 13); this occurs in 19 out of 26 metabolites in the activated region and 14 out of 26 metabolites in the deactivated region. This means that in more than 50% of the metabolites, there is a change in the pattern of value shifts between task and rest conditions in both regions. These data support the impact of the Faradarmani Consciousness Field on the brain metabolome of Faradarmangars within the time frame of this study.



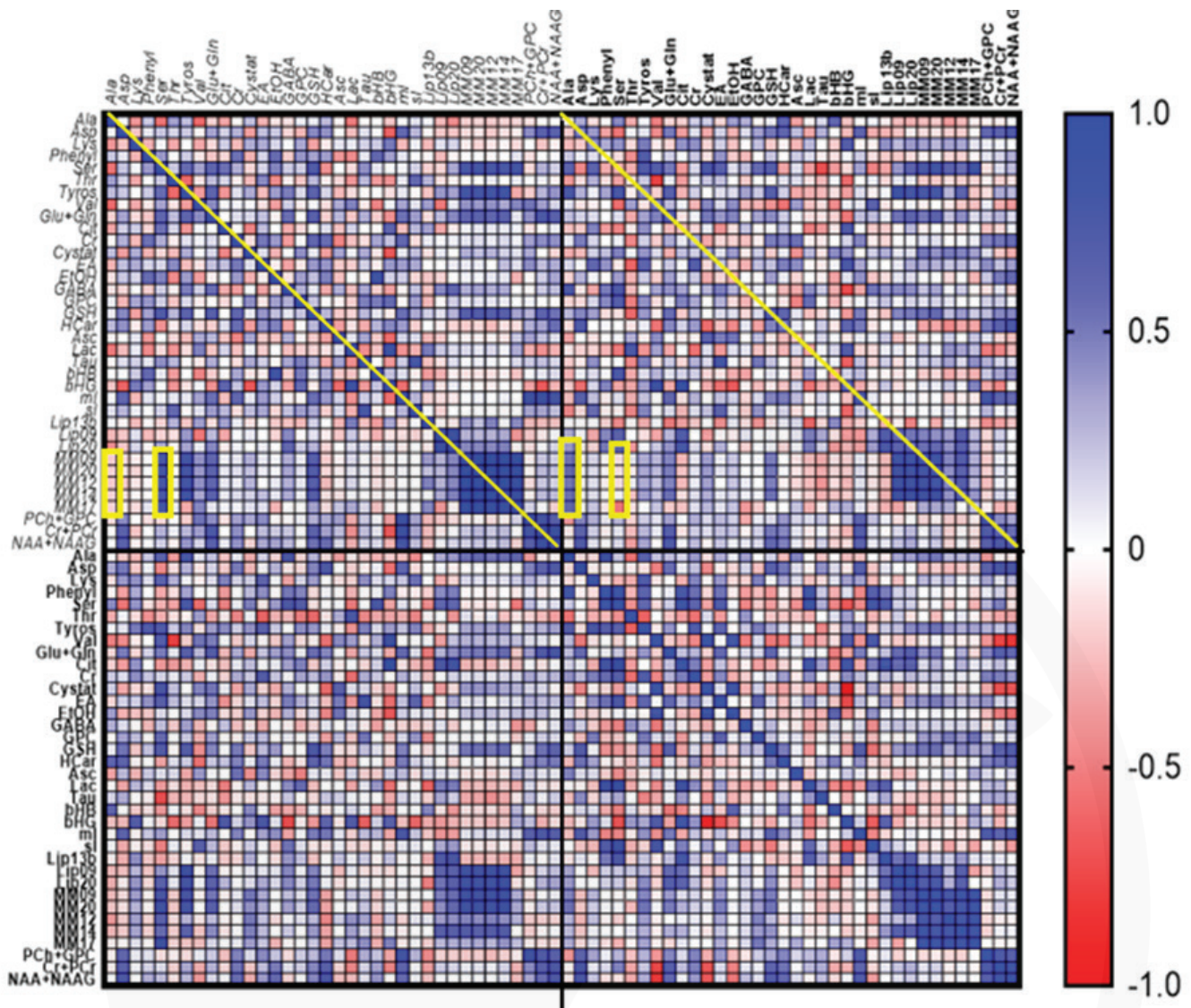


Figure 13. An overview of the changes in all metabolites examined across all studies in this issue under rest and task conditions in the activated (top) and deactivated (bottom) brain regions of Faradarmangars.

On the other hand, in the Pearson correlation analysis of all metabolites together, a distinct behavior—particularly within the macromolecule range—is observed in contrast to other metabolites (yellow boxes in Figure 13). Specifically, in the activated region and in the task vs. rest comparison, macromolecules exhibit not only significant changes in correlation within their own category (as also analyzed in direct comparisons), but also notable shifts in correlation with the amino acid threonine and the molecule GSH. In the deactivated region, considerable changes in the correlations between macromolecules and the amino acids serine and alanine are also evident. Furthermore, based on the lipid analysis in this region, notable correlation shifts are observed between Lip09 and Lip20 and the amino acid alanine. While these changes in

correlation, considering the previous significance analysis, are not independently conclusive, they are important in highlighting substantial fluctuations within the macromolecule group in relation to the brain–Faradarmani Consciousness Field interaction. This interaction appears to involve, in addition to the mentioned macromolecules, the amino acids threonine, serine, and alanine.

Conclusion

Overall, the change in Pearson correlation of the macromolecule set in the comparison between rest and task in both the activated and deactivated regions serves as a significant criterion for examining the effect of the Faradarmani Consciousness Field, particularly in the activated brain region. In

addition, specifically, the increase in the MM09 macromolecule and its negative correlation with other macromolecular metabolites in the activated region is another marker of the task in this area. Moreover, the change in correlation between macromolecules and the amino acids threonine (in the activated region), serine, and alanine (in the deactivated region) indicates a specific role of these amino acids in connection with the Faradarmani Consciousness Field in both studied regions. Moreover, a specific reference can be made to the reduced demand for and consumption of the ATP

molecule and its related metabolic pathways, as well as a notable shift in the energetics of brain cells, particularly in the activated region. Among these, the increase in lactate, ascorbate, and MM09 in these areas may support the enhancement of metabolic processes recorded in fMRI. On the other hand, in the deactivated region, without any significant changes, the decreasing trends of GPC and ascorbate and the increasing trends of PCh, glutamate, and Lip13b indicate a distinct metabolic response of this region compared to the activated region of the brain.

Acknowledgement

Authors would like to acknowledge Iranian National Brain Mapping Laboratory (NBML), Tehran, Iran for providing data acquisition service for this research work.

References

- Akiyama, Y., Yokoyama, R., Takashima, H., Kawata, Y., Arihara, M., Chiba, R., Kimura, Y., Mikami, T., & Mikuni, N. (2021). Accumulation of Macromolecules in Idiopathic Normal Pressure Hydrocephalus. *Neurologia medico-chirurgica*, *61*(3), 211–218. <https://doi.org/10.2176/nmc.oa.2020-0274>
- Alberini, C. M., Cruz, E., Descalzi, G., Bessières, B., & Gao, V. (2018). Astrocyte glycogen and lactate: New insights into learning and memory mechanisms. *Glia*, *66*(6), 1244–1262. <https://doi.org/10.1002/glia.23250>
- Ariyannur, P. S., Madhavarao, C. N., & Namboodiri, A. M. (2008). N-acetylaspartate synthesis in the brain: mitochondria vs. microsomes. *Brain research*, *1227*, 34–41. <https://doi.org/10.1016/j.brainres.2008.06.040>
- Barker, P. B., & Lin, D. D. M. (2006). In vivo proton MR spectroscopy of the human brain. *Progress in Nuclear Magnetic Resonance Spectroscopy*, *49*(2), 99-128. <https://doi.org/10.1016/j.pnmrs.2006.06.002>
- Beard, E., Lengacher, S., Dias, S., Magistretti, P. J., & Finsterwald, C. (2022). Astrocytes as Key Regulators of Brain Energy Metabolism: New Therapeutic Perspectives. *Frontiers in physiology*, *12*, 825816. <https://doi.org/10.3389/fphys.2021.825816>
- Benarroch E. (2024). What Is the Role of Lactate in Brain Metabolism, Plasticity, and Neurodegeneration?. *Neurology*, *102*(9), e209378. <https://doi.org/10.1212/WNL.0000000000209378>
- Bonilla, D. A., Kreider, R. B., Stout, J. R., Forero, D. A., Kerksick, C. M., Roberts, M. D., & Rawson, E. S. (2021). Metabolic Basis of Creatine in Health and Disease: A Bioinformatics-Assisted Review. *Nutrients*, *13*(4), 1238. <https://doi.org/10.3390/nu13041238>

Castellano, G., Dias, C. S., Foerster, B., Li, L. M., & Covolan, R. J. (2012). NAA and NAAG variation in neuronal activation during visual stimulation. *Brazilian journal of medical and biological research = Revista brasileira de pesquisas medicas e biologicas*, 45(11), 1031–1036. <https://doi.org/10.1590/s0100-879x2012007500128>

Chhetri D. R. (2019). *Myo-Inositol and Its Derivatives: Their Emerging Role in the Treatment of Human Diseases. Frontiers in pharmacology*, 10, 1172. <https://doi.org/10.3389/fphar.2019.01172>

Cudalbu, C., Behar, K. L., Bhattacharyya, P. K., Bogner, W., Borbath, T., de Graaf, R. A., Gruetter, R., Henning, A., Juchem, C., Kreis, R., Lee, P., Lei, H., Marjańska, M., Mекle, R., Murali-Manohar, S., Považan, M., Rackayová, V., Simicic, D., Slotboom, J., Soher, B. J., ... Mlynárik, V. (2021). Contribution of macromolecules to brain ¹ H MR spectra: Experts' consensus recommendations. *NMR in biomedicine*, 34(5), e4393. <https://doi.org/10.1002/nbm.4393>

Dossey, L. (2014). Spirituality and nonlocal mind: A necessary dyad. *Spirituality in Clinical Practice*, 1(1), 29–42. <https://doi.org/10.1037/scp0000001>

Dymek, A., Oleksy, Ł., Stolarczyk, A., & Bartosiewicz, A. (2024). Choline—An Underappreciated Component of a Mother-to-Be's Diet. *Nutrients*, 16(11), 1767. <https://doi.org/10.3390/nu16111767>

Hetherington, H., Petroff, O., Jackson, G. D., Kuzniecky, R. I., Briellmann, R. S., & Wellard, R. M. (2000). Magnetic resonance spectroscopy. *Magnetic Resonance in Epilepsy: Neuroimaging Techniques*, 333–384. <https://doi.org/10.1016/B978-012431152-7/50017-3>

Inazu M. (2019). Functional Expression of Choline Transporters in the Blood-Brain Barrier. *Nutrients*, 11(10), 2265. <https://doi.org/10.3390/nu11102265>

Koch, C., Massimini, M., Boly, M., & Tononi, G. (2016). Neural correlates of consciousness: progress and problems. *Nature reviews. Neuroscience*, 17(5), 307–321. <https://doi.org/10.1038/nrn.2016.22>

Lohrey, A., & Boreham, B. (2020). The nonlocal universe. *Communicative & integrative biology*, 13(1), 147–159. <https://doi.org/10.1080/19420889.2020.1822583>

Moffett, J. R., Ross, B., Arun, P., Madhavarao, C. N., & Namboodiri, A. M. (2007). N-Acetylaspartate in the CNS: from neurodiagnostics to neurobiology. *Progress in neurobiology*, 81(2), 89–131. <https://doi.org/10.1016/j.pneurobio.2006.12.003>

Nani, A., Manuello, J., Mancuso, L., Liloia, D., Costa, T., & Cauda, F. (2019). The Neural Correlates of Consciousness and Attention: Two Sister Processes of the Brain. *Frontiers in neuroscience*, 13, 1169. <https://doi.org/10.3389/fnins.2019.01169>

Nordström, L., Achanna, S., Naka, K., & Arulkumaran, S. (2001). Fetal and maternal lactate increase during active second stage of labour. *BJOG : an international journal of obstetrics and gynaecology*, 108(3), 263–268. <https://doi.org/10.1111/j.1471-0528.2001.00034.x>

Olufunmilayo, E. O., Gerke-Duncan, M. B., & Holsinger, R. M. D. (2023). Oxidative Stress and Antioxidants in Neurodegenerative Disorders. *Antioxidants*, 12(2), 517. <https://doi.org/10.3390/antiox12020517>

Oz, G., Alger, J. R., Barker, P. B., Bartha, R., Bizzi, A., Boesch, C., Bolan, P. J., Brindle, K. M., Cudalbu, C., Dinçer, A., Dydak, U., Emir, U. E., Frahm, J., González, R. G., Gruber, S., Gruetter, R., Gupta, R. K., Heerschap, A., Henning, A., Hetherington, H. P., ... MRS Consensus Group (2014). Clinical proton MR spectroscopy in central nervous system disorders. *Radiology*, 270(3), 658–679. <https://doi.org/10.1148/radiol.13130531>

Pessoa L. (2014). Understanding brain networks and brain organization. *Physics of life reviews*, 11(3), 400–435. <https://doi.org/10.1016/j.plrev.2014.03.005>

Rice M. E. (2000). Ascorbate regulation and its neuroprotective role in the brain. *Trends in neurosciences*, 23(5), 209–216. [https://doi.org/10.1016/s0166-2236\(99\)01543-x](https://doi.org/10.1016/s0166-2236(99)01543-x)

Rigotti, D. J., Inglese, M., & Gonen, O. (2007). Whole-brain N-acetylaspartate as a surrogate marker of neuronal damage in diffuse neurologic disorders. *AJNR. American journal of neuroradiology*, 28(10), 1843–1849. <https://doi.org/10.3174/ajnr.A0774>

Schwartz, J. M., Stapp, H. P., & Beauregard, M. (2005). Quantum physics in neuroscience and psychology: a neurophysical model of mind-brain interaction. *Philosophical transactions of the Royal Society of London. Series B, Biological sciences*, 360(1458), 1309–1327. <https://doi.org/10.1098/rstb.2004.1598>

Taheri, M. A., Torabi, S., Nabavi, N., Modarresi-Asem, F., Abbasi Sisara, M., Maftoun, P., & Semsarha, F. (2022). Task-fMRI Group and Functional Connectivity Analysis of the Brain During Faradarmani Consciousness Field Connection. *The Scientific Journal of CosmoIntel*, 1(2), 46–55. <https://doi.org/10.61450/joci.v1i2.29>

Trofin, D.-M., Sardaru, D.-P., Trofin, D., Onu, I., Tutu, A., Onu, A., Onită, C., Galaction, A. I., & Matei, D. V. (2025). Oxidative Stress in Brain Function. *Antioxidants*, 14(3), 297. <https://doi.org/10.3390/antiox14030297>

Veiga-da-Cunha, M., Chevalier, N., Stroobant, V., Vertommen, D., & Van Schaftingen, E. (2014). Metabolite proofreading in carnosine and homocarnosine synthesis: molecular identification of PM20D2 as β -alanyl-lysine dipeptidase. *The Journal of biological chemistry*, 289(28), 19726–19736. <https://doi.org/10.1074/jbc.M114.576579>

Wahbeh, H., Radin, D., Cannard, C., & Delorme, A. (2022). What if consciousness is not an emergent property of the brain? Observational and empirical challenges to materialistic models. *Frontiers in psychology*, 13, 955594. <https://doi.org/10.3389/fpsyg.2022.955594>

Yen, C., Lin, C.-L., & Chiang, M.-C. (2023). Exploring the Frontiers of Neuroimaging: A Review of Recent Advances in Understanding Brain Functioning and Disorders. *Life*, 13(7), 1472. <https://doi.org/10.3390/life13071472>

Zeisel, S. H., & da Costa, K. A. (2009). Choline: an essential nutrient for public health. *Nutrition reviews*, 67(11), 615–623. <https://doi.org/10.1111/j.1753-4887.2009.00246.x>